EFDA–JET–CP(10)06/38

M. Goniche, Y. Baranov, V. Basiuk, G. Calabro, A. Cardinali, C. Castaldo, R. Cesario, J. Decker, D. Dodt, A. Ekedahl, L. Figini, J. Garcia, G. Giruzzi, J. Hillairet, G.T. Hoang, A. Hubbard, E. Joffrin, K. Kirov, X. Litaudon, J. Mailloux, T. Oosako, R. Parker, V. Pericoli Ridolfini, Y. Peysson, P. Platania, F. Rimini, P.K. Sharma, C. Sozzi, G.Wallace and JET EFDA contributors

Lower Hybrid Current Drive for the Steady State Scenario

"This document is intended for publication in the open literature. It is made available on the understanding that it may not be further circulated and extracts or references may not be published prior to publication of the original when applicable, or without the consent of the Publications Officer, EFDA, Culham Science Centre, Abingdon, Oxon, OX14 3DB, UK."

"Enquiries about Copyright and reproduction should be addressed to the Publications Officer, EFDA, Culham Science Centre, Abingdon, Oxon, OX14 3DB, UK."

The contents of this preprint and all other JET EFDA Preprints and Conference Papers are available to view online free at www.iop.org/Jet. This site has full search facilities and e-mail alert options. The diagrams contained within the PDFs on this site are hyperlinked from the year 1996 onwards.

Lower Hybrid Current Drive for the Steady State Scenario

M. Goniche[1,8], Y. Baranov[2], V. Basiuk[1], G. Calabro[4], A. Cardinali[4], C. Castaldo[4], R. Cesario[4], J. Decker[1], D. Dodt[5], A. Ekedahl[1], L. Figini[7], J. Garcia[1], G. Giruzzi[1], J. Hillairet[1], G.T. Hoang[1], A. Hubbard[3], E. Joffrin[8], K. Kirov[2], X. Litaudon[1], J. Mailloux[2], T. Oosako[1], R. Parker[3], V. Pericoli Ridolfini[4], Y. Peysson[1], P. Platania[7], F. Rimini[8], P.K. Sharma[6], C. Sozzi[7], G.Wallace[3] and JET EFDA contributors*

JET-EFDA, Culham Science Centre, OX14 3DB, Abingdon, UK

[1]CEA, IRFM, F-13108 Saint Paul-lez-Durance, France
[2]EURATOM/CCFE Fusion Association, Culham Science Centre, OX14 3DB, Abingdon, OXON, UK
[3]MIT Plasma Science and Fusion Center, Cambridge, MA, USA
[4]Associazione EURATOM-ENEA sulla Fusione, Via E. Fermi 45, 00044 Frascati, Roma, Italy
[5]Max-Planck Institut für Plasmaphysik, Euratom Association, Garching, Germany
[6]Institute for Plasma Research, Bhat, Gandhinagar – 382428, India
[7]Associazione EURATOM-ENEA, IFP-CNR, Via R. Cozzi, 53 20125 Milano, Italy
[8]JET-EFDA-CSU, Culham Science Centre, OX14 3DB, Abingdon, OXON, UK
** See annex of F. Romanelli et al, "Overview of JET Results",*
(Proc. 22 [nd] IAEA Fusion Energy Conference, Geneva, Switzerland (2008)).

Preprint of Paper to be submitted for publication in Proceedings of the
37th EPS Conference on Plasma Physics, Dublin, Ireland.
(21st June 2010 - 25th June 2010)

ABSTRACT.
Lower Hybrid Current Drive (LHCD) experiments performed at density close to that required for the steady state scenario are reported. On C-Mod, FTU and Tore Supra, a strong decay of the brehmsstrahlung emission is observed when the density is increased, much faster that the prediction of LHCD modelling. On JET, LH power deposition is also found to be sensitive to the plasma density: LH power modulation indicates that the power deposition moves to the very edge of the plasma ($r/a \sim 0.9$) when the density approaches the requirement of the JET SS scenario. From this experiment but also from the reconstruction of the electron cyclotron emission spectrum, the decrease of the LHCD efficiency with density is also found. From LHCD modelling of different JET pulses performed at different densities and wave parallel refraction indexes, it is concluded that the wave accessibility condition is not the key parameter for explaining the decrease of the efficiency. C-Mod, FTU and Tore Supra experiments indicate that the plasma edge parameters, namely density and temperature but also fluctuations, are affecting the efficiency via loss mechanisms which are likely to be collisional damping (C-Mod), parametric decay instabilities or wave scattering (FTU/ Tore Supra).

1. INTRODUCTION

Lower hybrid range of frequency waves have shown their ability to drive efficiently the toroidal current on many tokamaks. Lower Hybrid Current Drive (LHCD) has been used successfully in the plasma ramp-up phase or in the plateau high power phase of the discharge for two main purposes: volt-second saving and current profile modification. Most of the experiments have been carried out at relatively low plasma density, while the development of the steady state scenario for ITER require high densities, typically a volume-averaged density $\langle n_e \rangle = 7\times10^{19}\ m^{-3}$. On JET, development of the steady State Scenario (SS) with LHCD cannot be performed as such high density because of the much lower toroidal field (~3T compared to 5.3T on ITER). The so-called 'wave accessibility condition', which scales with fpe/fce (where fpe is the electron plasma frequency and fce the electron cyclotron frequency), imposes a density not exceeding $\langle n_e \rangle \sim 3.5\times10^{19}\ m^{-3}$. In a complementary way, the field of FTU (up to 8T) and C-Mod (up to 7T) allows LHCD experiments at densities exceeding $1\times10^{20}\ m^{-3}$. In these machines, the LHCD efficiency was characterized in a wide range of densities from the multi-chord Hard X-Ray diagnostic. On Tore Supra which has a field (3.85T) slightly higher than JET, the density at the plasma edge was modified independently of the mean plasma density which was varied up to $\langle n_e \rangle = 5.5\times10^{19}\ m^{-3}$.

In this paper after a review of the requirement of the steady state scenario (section 2) and of the LHCD results achieved in past experiments (section 3), we will report on the LHCD experiments performed on FTU, C-Mod and Tore Supra at density close (or exceeding) the density required for the ITER SS scenario, with emphasis on the effect of the temperature and density of the plasma edge on the current drive efficiency (section 4). Section 5 is devoted to the analysis of two JET SS scenario pulses performed with different margins with respect to the accessibility condition. The Electron Cyclotron Emission (ECE) was confronted to the LH-driven current computed from a ray tracing/

Fokker-Planck code. From these experimental results associated to LHCD (and ECE) modelling, implications for LHCD on ITER are given in section 6, before the conclusion (section 7).

2. THE STEADY STATE SCENARIO

The steady state requires for a tokamak a fully non-inductive discharge, i.e. a toroidal current fully driven by external sources or by the neoclassical bootstrap mechanism ('the bootstrap current' IBS). This scenario is characterized by a lower plasma current ($I_p = 9$MA) and a lower plasma density ($<n_e> = 7\times10^{19}$ m^{-3}) with respect to the baseline scenario [22]. The ITER SS scenario is aiming at maintaining a $Q = 5$ plasma for 3000s. This requires the bootstrap current to account for at least ~50% of the total current. Such high ratio IBS/Ip requires high normalized plasma pressure $\beta_N \sim 3$ combined with high confinement factor H~1.6 compared to the values of the baseline scenario ($\beta_N = 1.8$, $H = 1.0$). The MHD stability of such discharges can be achieved with a negative magnetic shear leading to a hollow safety factor profile with a minimum q larger than 2. Various scenarios have been proposed from weak to strong magnetic shear but they all require off-axis (r/a>0.6) current drive sources. High frequency waves (ICRF, LHRF, ECRF) can in principle provide this source but lower hybrid waves are the best candidate thanks to their high current drive efficiency. A scenario using only HF waves for heating and current drive has been recently proposed [16]. Whereas EC waves (20MW) drive the current at r/a~0.45 aligned with the bootstrap current, the LH-driven current provided by 13MW of power, is more off-axis at r/a~0.7 (figure 1). It results in a strongly negative magnetic shear with enhanced confinement ($H = 1.7$, $\beta_N \sim 3$) and the discharge is maintained for 3000s with $Q = 5$ ($I_p = 9$MA, $<n_e> = 7\times10^{19}$ m^{-3}). However this scenario is not MHD stable and was further improved by reducing the negative magnetic shear in the core [17].

Candidates for the SS scenario have been developed on many tokamaks and for some of them (JET, JT60-U, Tore Supra), LHCD has been used for shaping the current profile. On JET, application of a moderate LH power (~2MW) in the plasma current ramp-up phase (LHCD prelude) was found to be very efficient to achieve highly negative magnetic shear. This leads to the formation of an internal transport barrier at wide radius and access to improved core confinement is obtained with a reduced heating and current drive power as inferred from comparing the neutron yield of discharges with LHCD prelude to that of discharges with no LHCD prelude (figure 2) [9] .

3. LOWER HYBRID CURRENT DRIVE: THEORY AND RESULTS OF EARLIER EXPERIMENTS

3.1. THEORETICAL BASIS FOR THE LHCD EFFICIENCY

Lower Hybrid Current Drive relies on the Landau damping of high phase velocity waves travelling in the direction of the plasma current [12]. The high current drive efficiency, which is the ratio of the driven current density j_{LH} to the absorbed power density p_{LH}, results from the low collisionality of the resonant electrons. Very simply, by considering that for maintaining an electron current density $j_{LH} = n_e e v_{||}$ the electron kinetic energy density $n_e m_e v_{||}^2/2$ must be 'refreshed' on a characteristic time of the order of the collision time ν_{col}, the efficiency can be written as $j_{LH}/p_{LH} \sim e/(m_e v_{||} \nu_{col})$.

For high velocity electrons, $\nu_{col} \sim 1/v_{||}^3$, and the efficiency scales as $v_{||}^2 \sim 1/N_{||}^2$, $N_{||}$ being the parallel refractive index of the wave with which the electrons are resonant. It results a deformation of the initial Gaussian electron function distribution with a plateau for electrons having a velocity $v1<v_{||}<v^2$ carrying the driven current (figure 3).

Assuming that the diffusion coefficient in the velocity space $D(v_{||})$ is very large on the plateau and 0 elsewhere, the 1D steady-state Fokker- Planck equation can be solved analytically. In the high velocity limit, a $1/(5+Z_{eff})$ dependence is found for the efficiency [13]. When a homogeneous (in space) driven current, density and absorption power are considered, the normalized CD efficiency $\eta = n_e R I_{LH} P_{LH}$ (n_e plasma density, R major plasma radius, I_{LH} driven current, P_{LH} absorbed LH power) is found to depend not only on $N_{||}$ and Z_{eff} but also on Te, with typically an efficiency increasing by a factor 2 when the temperature is increased from 5 to 20keV [30]. It should be noted that the absorbed power is generally quoted in theoretical papers but experimental efficiency is generally obtained from the coupled power which means that the considered power includes the secondary $N_{||}$ lobes (~30% of the power) of the excited spectrum which are less efficient to drive current.

These dependencies were experimentally found and in particular the increase of efficiency with T_e was verified on Asdex, JT-60, JT-60U [50] and on JET [3]. A simple scaling, expressed by $\eta = 12 <T_e>/(5+Z_{eff})$, could reasonably well fit the data [28].

Assuming that the wave undertakes a $N_{||}$ upshift close to the Landau damping limit $v_{||}/v_{th} = 2.7$, this linear dependence with Te is explained [49]. From this analysis, the theoretical limit given by Karney and Fisch [30] is retrieved at very high temperature. Other empirical scaling laws have been proposed from FTU [38] and Tore Supra [19] experiments, indicating for these limiter machines with a more peaked temperature profile a weaker $<T_e>$ dependence, close to $<T_e>0.5$. It is also found a beneficial effect of Ip which is closely linked to Te in discharges with LH waves only for heating and current drive. In both these experiments impurity effect close to the $1/(Z_{eff}+5)$ scaling factor is also found.

3.2 COUPLING, PROPAGATION AND ABSORPTION OF THE LH WAVE

Starting from the launching structure (the antenna), the wave can be coupled to the plasma if the density exceeds the cut-off density (which is equivalent to say that the electron plasma frequency wpe must be larger that the wave frequency). This cut-off density which scales like the square of the frequency is in the $2\text{-}8\times10^{17} m^{-3}$ range for a frequency in the 3.7-8GHz range. This condition is generally fulfilled naturally in the Scrape-Off Layer (SOL) but can be critical in particular in H-mode discharges and requires sometimes particle fuelling near the antenna for rising the density by local LH-induced ionization [11, 21].

The wave can then propagate into the plasma as long as the density is lower than a critical value which depends on the local value of the electron density and magnetic field. This limit called the 'accessibility condition' can be expressed as $N_{||} > N_{||,\,acc}$ where $N_{||,\,acc}$ is a function of the ratio of the plasma frequency to the electron cyclotron frequency. During the toroidal propagation, the wave undergoes a change of its phase velocity as illustrated in figure 4, showing the ray tracing for

a SS scenario JET pulse. Rays are launched from different poloidal locations, corresponding to different waveguide rows, and the $N_{||}$ of these rays evolves differently during the propagation but keeps fulfilling the accessibility condition.

Strong Landau absorption condition occurs when the temperature of the plasma is such that the population of resonant electrons is large enough. This condition writes $N_{||}>6.5/T_e^{1/2}$ or alternatively $v_{||}/v_{th} < 3.5$. In present tokamaks, this condition is not fulfilled for the launched $N_{||}$ value which should be as low as possible for maximizing the efficiency but is constrained by the accessibility condition and lies between 1.5 and 2.5, imposing a temperature $T_e \sim 10$keV. By quasi-linear diffusion in the velocity space, the 'spectral gap' is filled and the plateau is extended from the condition $v_{||}/v_{th} = 3.5$ to $v_{||}/v_{th} = 10$ for the case of the pulse shown in figure 3.

In the weak absorption case, the rays undergo several reflections (typically 3-8 for a JET steady state scenario case) at the plasma boundary (figure 5). Although the validity of the geometrical optics is questionable when the wavelength is large (the wavelength goes to infinity when the density approaches the cut-off density at the plasma edge), full-wave simulations have shown that the ray-tracing approach gives a satisfactory description of the wave propagation at least in the few cases where the comparison was made [52].

3.3 POWER LOSS CHANNELS IN THE SCRAPE-OFF LAYER

In the scrape-off layer (and near the separatrix), several mechanisms can be responsible either for a change of the $N_{||}$ spectrum or for a LH power absorption both leading to a reduction of current drive efficiency.

The launched $N_{||}$ spectrum, apart from the main peak $N_{||0}$ (~2), is composed of many harmonics which amplitude roughly decays with their order. The very high order harmonics ($|N_{||}| > 30$) can be damped by Landau effect on thermal electrons ($T_e \sim 20$eV) in the SOL. When diffusing in the velocity space, these electrons can interact with lower and lower harmonics [14, 15]. Power losses were experimentally observed from hot spots on plasma facing components magnetically connected to the LHCD antenna but because of the limited power available from these harmonics, the dissipated power cannot exceed 10% and experimental measurements indicate less than 5% in good coupling conditions [18].

Parametric Decay Instabilities (PDI) were a major concern when LH waves were used for ion heating with the operating frequency (ω_0) very close to the lower hybrid frequency (ω_{LH}) [44] and in early LHCD experiments performed at high density ($1<\omega_0/\omega_{LH}<2$) [26]. These instabilities are originated from mode coupling between the launched wave w0 and low frequency waves w in the ion sound or the ion cyclotron frequency range of frequency [43, 45, 5]. It results in sidebands modes ($\omega_0 \pm \omega$) and spectral broadening of the launched wave, both being been experimentally measured on several tokamaks. By solving the dispersion relation, the growth rate and frequency of these instabilities can be computed but attention has to be paid for ordering correctly the terms of the field equation [36, 35]. For JET SS pulses performed at relatively low plasma density ($<n_e> = 2\times10^{19}$ m^{-3}, $\omega_0/\omega_{LH}>4$), the PDI modelling predicts the growth of the ion sound quasi-mode (ω/ω_0

$= 1\text{-}2\times10^{-3}$) and a distortion of the $N_{||}$ spectrum with 10% of the power being transferred to a tail extending up to $N_{||} \sim 3$ [6] (figure 6). It results a more peripheral power deposition profile which, in this case, is favourable for sustaining the high confinement regime.

Scattering of the launched wave by density fluctuations, which is also a 3-wave problem, has also been invoked as a possible mechanism for reducing the LHCD efficiency [1]. Spectral broadening is also expected and correlation between LHCD efficiency, spectral broadening and density fluctuations has been reported on Asdex [37].

For high density and low temperature at the plasma edge, electron-ion or electron-neutral collisions can significantly contribute to wave damping. By simply including a friction force in the motion equation of a test particle, it can be shown that the damped power scales as $(\nu/\omega)^2$ where n is the collision frequency. On NSTX, when $\nu/\omega > 10^{-4}$, electron Bernstein wave was damped, but this effect is mitigated by evaporated lithium conditioning which reduces the density at the plasma edge [10]. Comparing the normalized collision frequency of the plasma n/w for JET, C-Mod and ITER, this effect is expected to be important for C-Mod which has a low temperature and high density in the SOL (typically $T_e < 10$eV and $n_e \sim 1\times10^{19}$ m^{-3} behind the last closed flux surface) and weak for JET (figure 7).

4. LHCD EXPERIMENTS AT DENSITY CLOSE TO THE ITER SS SCENARIO REQUIREMENT

LHCD experiments were carried out at high density up to $\bar{n}_e = 2.2\times10^{20}$ m^{-3} in FTU, $\bar{n}_e = 1.5\times10^{20}$ m^{-3} in C-Mod and $\bar{n}_e = 0.6\times10^{20}$ m^{-3} in Tore Supra. From the relative loop voltage drop (DV/V), the estimate of the current drive efficiency is uncertain when DV/V is lower than 50% as in these reported experiments. Instead the bremsstrahlung emission in the Hard X-Ray (HXR) energy range (40-200keV) which is known to be well suited for diagnosing the LH-induced fast electron population has been used for these experiments. However, the LH-driven current (ILH) cannot be reconstructed from the tomography of the bremsstrahlung emission provided by a multi-channel diagnostic. A possible approach is to reconstruct the HXR emission from the computed electron function distribution and to compare to experimental signals [41, 51]. Nevertheless a very rough estimate of the density dependence of the HXR emission can be done. For the electron-ion bremsstrahlung, the emission IHXR is proportional to the fast electron density n_f, the electron density ne and a function depending on the ions charge which can be approximated by Z_{eff}. Assuming a constant LHCD efficiency (and neglecting the Z_{eff} dependence of the efficiency) $n_f \sim 1/n_e$ and IHXR~Z_{eff}.

We present here the line-integrated HXR emission as a function of the line- (or volume-) averaged electron plasma density for these three machines. These signals provide an insight to the evolution of the LHCD efficiency with density which has been compared in one case with the reconstructed signals.

4.1 EFFECT OF THE EDGE TEMPERATURE (FTU)

On FTU which is a circular limiter machine ($R/a = 0.935/0.285$m, $I_p \leq 0.7$MA), the HXR emission

(40-200keV) falls off rapidly when the line-averaged density is varied between $\bar{n}_e = 0.7$ and 1.4×10^{20} m^{-3} and no signal above noise level is detected for $\bar{n}_e > 1.2\times10^{20}\ m^{-3}$. By changing the scenario, HXR emission is recovered for densities up to $\bar{n}_e > 2\times10^{20}\ m^{-3}$ [8] (figure 8). This is obtained by combining the use of a small wetted surface lithium limiter on low field side with pellet injection for particle fuelling. Note however that this increase of HXR emission is obtained transiently. Two main observations could be done during these experiments: i) the temperature in the outer part ($0.65 \le r/a \le 0.95$) of the plasma is much larger ($\times$1.5-2) for the high HXR emission case and this temperature which varies during the LHCD pulse is correlated to the HXR emission ii) the spectral broadening of the launched wave (0.35-0.53MW at 8GHz) is reduced from 15 to 7MHz (measured at $-$45dB). From the LHstar code [7], the growth rate of the parametric decay instabilities is found to be reduced for the high temperature case. This spectral broadening can be alternatively explained by density fluctuations in the SOL and applying the Andrews' model, the computed spectral broadening, using density fluctuations measurement in the SOL, is in good agreement with the measurement for a wide range of values. The resulting loss of power in the SOL is consistent with the HXR emission measurements [39].

4.2 DENSITY DEPENDENCE FOR HIGHLY COLLISIONAL PLASMA EDGE (C-MOD)

The HXR emission (40-200keV) is also found to decay very strongly with the plasma density on C-Mod ($R/a = 0.67/0.20$m, $I_p \le 1.5$MA, divertor elongated discharges). By varying the density between $\bar{n}_e = 0.5\times10^{20}\ m^{-3}$ and $1.5\times10^{20}\ m^{-3}$, the emission can decrease by three orders of magnitude [51] (figure 9). Reconstruction of the signals from the Fokker-Planck code CQL3D [23] indicates a dependence close to $1/\bar{n}_e$ for these discharges, which is likely to result mainly from a dilution effect (Z_{eff} decreases from 3 to 1.5). By including collisional damping in the code, the experimental strong decay is qualitatively reproduced. For these discharges where w/wLH varies from 4.6 to 3.2, the strongest sideband is below $-$20 dB relative to the launched wave (0.55-0.9MW at 4.6GHz), corresponding to less than 1%. Moreover comparison of data at 5.4T and 7.0T shows that bremsstrahlung emission does not scale with ω/ω_{LH} and PDI are not expected to contribute significantly to the LHCD efficiency reduction at high density.

4.3 EFFECT OF THE PARTICLE FUELLING (TORE SUPRA)

Similar to FTU and C-Mod experiments, a strong decay of the HXR emission (60-120keV) with the volume-averaged plasma density $\langle n_e \rangle$ is found on Tore-Supra ($B_t = 3.85$T, $R/a = 2.38/0.72$m, $I_p \le 1.5$MA, limiter circular discharges), with a scaling close to $1/\langle n_e \rangle^3$ (figure10). This density scaling is confirmed by analyzing a larger data base [46]. Two different limiter configurations were tested: large bottom toroidal limiter and small low field side limiter, but no change in the HXR emission could be detected although the recycling was much higher in the second case. In the first case, when the distance between the antenna and the LCFS is varied from 4 to 8cm, the HXR emission does not change. For these different configurations, the edge temperature, measured by the Thomson scattering diagnostic, does not change ($T_e(r/a = 0.96) \sim 150$eV for $\langle n_e \rangle = 5.2\times10^{19}\ m^{-3}$) which is

consistent with the FTU results. In contrast, a beneficial effect of pellet fuelling, with respect to gas fuelling, is found when the density exceeds $<n_e> = 4.5\times10^{19}\ m^{-3}$, leading to an increase of the HXR emission by a factor 2-3 at $<n_e> = 5.5\times10^{19}\ m^{-3}$. For the pellet-fuelled discharge at a rate of 3Hz, the LH power is notched at the same frequency in order to avoid pellet ablation at the edge by the generated fast electrons, therefore LHCD at very high density is achieved only transiently. For the same couple of pulses, the turbulence is evaluated from the saturation current of a Langmuir probe embedded in the LHCD antenna. For the gas-fuelled pulse, the fluctuation rate increases by more than one order of magnitude when the density is increased by 30% whereas the turbulence level is kept at low level for the pellet-fuelled pulse in the entire density range (figure 11). It should be noted however, that this difference does not reflect exactly HXR emission of pellet-fuelled pulse which departures significantly from the gas-fuelled pulse only for $<n_e> > 4.5\times10^{19}\ m^{-3}$.

5. MODELLING OF JET PULSES IN THE STEADY STATE SCENARIO

Whereas previous experiments of the SS scenario on JET were performed at relatively low plasma density [34, 29, 6] or at higher density ($n_e(0)\sim 6\times10^{19}\ m^{-3}$) but with a density at the top of the pedestal not exceeding $n_{e,ped}\sim2.5\times10^{19}\ m^{-3}$ [48, 32], new experiments were performed at higher power ($P_{tot}\sim 30$MW) with a density at the pedestal $n_{e,ped}\sim3.5\times10^{19}\ m^{-3}$. These discharges are also characterized by higher temperature at the pedestal ~2keV instead of ~1.2keV.

On JET, the high neutron rate makes impossible the use of the bremsstrahlung emission diagnostic. Therefore, in order to investigate the density dependence of the LH deposition and current drive efficiency, a LH power modulation technique is used. The amplitude and phase response of the electron temperature, measured with the Electron Cyclotron Emission (ECE) diagnostic, allows to determine the localization in radius of the LH power deposition [31]. Furthermore Fokker-Planck analysis shows that the ratio between the amplitudes of the third and the main harmonics, $\delta Te_3/\delta Te_1$, is strongly affected by the width of the quasi-linear plateau, and therefore the LHCD efficiency. When the density $\bar{n}_e$ increases from $1\times10^{19}\ m^{-3}$ to $3.5\times10^{19}\ m^{-3}$ the power deposition moves more off-axis from r/a~0.5 to r/a~0.9 (figure 12). At the same time, the normalized width of the plateau $\Delta=(v_2-v_1)\ v_{th}$ shrinks from $\Delta\sim6$ to $\Delta\sim2$. Most of these experiments were carried out in low temperature L-mode plasmas, but the two pulses performed in H-mode (in the upper right corner of figure 12) follow the same trend.

Two SS scenario JET pulses were analyzed in detail with the CRONOS suite of codes [2] which includes the C3PO-LUKE code for the LHCD part.. These pulses were performed with comparable LH power, ~2.5MW for Pulse No: 77895 and 2MW for Pulse No: 72835, but with different launched $N_{||}=2.1$ for Pulse No: 7895 and $N_{||}=2.3$ for Pulse No: 72835. The plasma parameters were almost identical: $B_t=2.7$T, $I_P=1.8$MA, $<n_e>\sim3.8\times10^{19}\ m^{-3}$, $n_{e,r/a=0.8}>\sim3.5\times10^{19}\ m^{-3}$, except for the electron temperature which is higher for Pulse No:77895 ($<T_e>\sim 3$keV) than for Pulse No: 72835 ($<T_e>\sim$ 2.3keV). The loop voltage was ~50mV and ~100mV. The $N_{||}$ spectrum was computed from the LH coupling code ALOHA [24] and in addition to the main lobe, 5 secondary lobes were considered for the ray tracing and Fokker-Planck codes. Rays were launched from 6 poloidal locations to take

into account the antenna extension, leading to a total of 36 rays. From the density profiles measured by the high resolution Thomson scattering system for the confined plasma and the lithium beam diagnostic for the edge and the SOL, the minimum value of the N// which is accessible can be computed. For the low $N_{||}$ case ($N_{||} = 2.1$), the wave is found to be marginally accessible whereas the high $N_{||}$ case ($N_{||} = 2.3$) fulfils the good accessibility condition (figure13).

For the marginal accessibility case, the ray trajectory is very sensitive to both the poloidal launch position and the kinetic profiles. It results in a power deposition varying considerably from one time to another (figure 14-a). In the case of good accessibility, the ray trajectory is much more stable (figure 14-b) but in both cases, a broad power deposition (and density of driven current) in the outer part of the plasma is obtained (r/a = 0.4-0.9 for the first case, 0.5-0.85 for the second one) and a total stable driven current (~0.15MA for the first case, ~0.10MA for the second one). In spite of the weak accessibility condition for the low $N_{||}$ case, the LHCD efficiency is larger ($\eta \sim 0.9\times10^{19}$ $A.W^{-1}m^{-2}$) compared to that of the high $N_{||}$ case ($\eta \sim 0.6\times10^{19}$ $A.W^{-1}m^{-2}$). This demonstrates that the accessibility condition does not play a major role for these shots and that the efficiency is related to the launched N// value and the plasma temperature. In order to further assess the role of the accessibility condition, these results were compared to a L-mode pulse (Pulse No: 74087) performed at lower plasma density ($n_{e,\,r/a=0.8} > \sim 3.5\times10^{19}m^{-3}$) but with a lower $N_{||} = 1.8$ and lower magnetic field ($B_t = 2.46T$) leading to a comparable accessibility to that of Pulse No: 77895 (figure 13). In that case, the power deposition is also unstable and very broad (figure 14-c). The LHCD efficiency for this low temperature plasma ($<T_e> \sim 1.1keV$) is found to be very similar to that of Pulse No: 77895 ($\eta \sim 1.0\times10^{19}$ $A.W^{-1}m^{-2}$) but still below the scaling law by a factor 1.9. Comparing the LHCD efficiency of these two pulses performed with poor accessibility conditions, the effect of $N_{||}$ clearly prevails on the effect of T_e.

This broad power deposition in the outer part of the plasma (r/a = 0.4-0.9) obtained for the SS scenario pulses is not fully consistent with the modulation experiment indicating a power deposition peaked at r/a~0.9 (figure 12). The growth rate of parametric decay instabilities and the resulting $N_{||}$ spectrum crossing the separatrix were computed for Pulse No: 72835. This modified spectrum with a tail extending up to $N_{||} = 4$ leads to a very peripheral power deposition ($r/a \sim 0.95$) which seems more consistent with the modulation experiment.

For estimating the current drive provided by the LH waves, magnetic measurements do not provide any quantitative information as the computed magnetic flux saving is less than 0.1V.s for 4s of LHCD and the internal inductance reduction less than 0.02 which. Both values arewithin the error bars of these measurements.

The ECE diagnostic has the capability of detecting a very small fraction of the electron distribution when these electrons are sufficiently energetic to perturb the ECE of the thermal contribution with the cold resonance outside the plasma. On JET, this occurs for the down-shifted second harmonic for electrons of energy E > 60keV when located in the plasma at R > 3.4m (r/a > 0.35). This condition is expected to be fulfilled for the medium to high density pulses. The oblique ECE diagnostics of JET provides five simultaneous spectra (nominally 0^o X mode, 10^o and 20^o X and O modes, where the

angle refers to the radial direction) over an extended frequency range (70-350GHz), with spectral resolution up to 7GHz and time resolution of 5ms [47]. The ECE spectrum was first reconstructed from a pure thermal plasma with no LH tail and then assuming a fast electron population (figure 15). From accurate determination of the experimental error bars, it is concluded that for Pulse No: 77895, a minimum density fraction of suprathermal electrons $\eta_0 = 0.8\times10^{-4}$ can be detected. Assuming a Gaussian distribution of these electrons centred on r/a = 0.5 (resp. 0.6) with a full width at $1/e^2$ height Δ(r/a) = 0.3, the maximum LH driven current is estimated to be 43kA resp. 71kA) [42]. We conclude that there is a discrepancy with the LHCD modelling, predicting I_{LH}~150kA, by at least a factor 2. Doing the same analysis for the medium density pulse, whose ECE spectra have a large peak at the down-shifted 2nd harmonic (f~100GHz), the spectra are satisfactorily modelled with $\eta_0 = 1.2\times10^{-3}$ and LH power deposition at r/a = 0.75 with a full width D(r/a) = 0.35. The corresponding LH current is 0.40MA which is in reasonable agreement with the LHCD modelling, indicating 0.60MA for this 5MW pulse.

6. PROSPECTS FOR ITER

A high pedestal temperature is required to achieve a high energy multiplication factor. The electron temperature at r/a=0.65 should reach 10keV for the SS scenario. As a result, waves, with a launched $N_{||}$ = 1.9-2.0, will be absorbed at the first pass (strong Landau damping condition) at a normalized radius r/a = 0.6-0.7 (figure 17). Taking into account the full $N_{||}$ spectrum launched by the antenna, the LHCD efficiency is computed to be $\eta \sim 1.5\times10^{19}$ A.W^{-1}m^{-2} and the driven current to be $I_{LH} \sim$ 0.7MA with 20MW of coupled LH power [25].

The kinetic profiles of the ITER SOL are still uncertain which makes the predictions for LH power absorption difficult. The ITER SOL is very large (~0.20m) and for the far SOL ($R-R_{sep} >$ 0.04m) modelling is based on convective turbulent transport with a velocity in the 30-100m/s range [Loarte08]. In the close SOL where the transport is assumed to be diffusive and leading to steep profiles, the temperature is expected to drop from $T_e \sim 200$eV at the LCFS to T_e = 7-10eV in 5-7cm and consequently in the high radial convective velocity case the normalized collisionality n/f can be large (figure 7). However collisional absorption should be marginal for single-pass absorption of the LH wave. There is still an issue on PDIs and fluctuation scattering. High growth rate of PDIs and reduction of LHCD efficiency is expected for too low temperature in the SOL. The fluctuation level in the SOL is unknown and the large width of the SOL, which may require local gas injection, for LH coupling control, could be unfavourable. hooowever LHCD experiments at low density on JET have shown that neither the LHCD nor the density fluctuation rate at the plasma periphery were affected when the antenna-LCFS distance (up to 0.09m) or local gas injection rew increased [20]. LHCD experiments performed at high density did not either show effect of the gap (up to 0.08m) on the efficiency.

CONCLUSIONS

LHCD experiments performed on C-Mod, FTU and Tore Supra in L-mode discharges indicate a

degradation of the current drive efficiency when the plasma density is increased. This observation is related to edge plasma parameters, namely the density and the temperature, and different mechanisms can be involved: collisional absorption, parametric decay instabilities, wave scattering on density fluctuations. The dominant process can vary from one experiment to another.

On JET, in L-mode discharges, the power deposition is found to move to the very edge (r/a~0.9) when the density approaches the condition of the JET SS scenario. Reduction of the CD efficiency is also inferred from these LH power modulation experiments. The few pulses performed with this scenario but in H-mode confirm this trend. Comparing discharges performed with different values of launched N// values and densities, it is assessed that the accessibility condition, which is marginally fulfilled for the developed SS on JET, is not the main parameter in order to explain the reduction of CD efficiency. Reconstruction of the ECE spectra indicates that the computed CD efficiency is too large by at least a factor 2 whereas the power deposition is correctly modelled for a medium density case giving confidence in the ECE modelling. When collisional absorption in the edge is included in the modelling, no more than 10% of the power is lost for the high density pulse and this mechanism is excluded for explaining the reduction of LHCD efficiency. These results should be confirmed by new experiments performed at higher field (improve the wave accessibility) and higher LH power (reduce the uncertainty on the ECE modelling). The new metallic wall will change the particle recycling and ne/Te profiles in the edge could be beneficially changed. From FTU and Tore Supra results, particle fuelling with pellets should also be beneficial.

On ITER the single-pass absorption scheme gives more confidence in the ray tracing/ Fokker-Planck codes and with proper shaping of the $N_{||}$ (=1.9-2.0), the power is expected to be deposited at a normalized radius r/a = 0.6-0.7 with a good CD efficiency although significantly lower than the one expected from the JT60-U scaling. In order to quantify the power loss in the SOL, more accurate data on the ne/Te profiles (average values and fluctuations) are required.

ACKNOWLEDGMENTS

This work, supported by the European Communities under the contract of Association between EURATOM and CEA, was carried out within the framework of the European Fusion Development Agreement. The views and opinions expressed herein do not necessarily reflect those of the European Commission.

REFERENCES

[1]. P.L. Andrews,V.S. Chan, C.S. Liu, Physics of Fluids **28** (1985) 1148

[2]. Artaud J.F., Basiuk V., Imbeaux F., et al., Nuclear Fusion **50**, 043001 (2010)

[3]. Y. Baranov, A. Ekedahl, P.Froissard, C. Gormezano, M. Lennholm, F.Rimini, F. Söldner, Nuclear Fusion **36** (1996)1031-1046

[4]. A.Cardinali , Physics of Plasmas, **14** (2007)112506

[5]. Cesario R. and Cardinali A., Nuclear Fusion **29** (1989) 1709

[6]. Cesario R., Cardinali A., Castaldo C., Paoletti F. and Mazon D., Physics Review Letters, **92** (2004) 175002

[7]. R. Cesario, Nuclear Fusion **46** (2006) 462–476
[8]. Cesario R. , L Amicucci, A Cardinali, C Castaldo, M Marinucci, L Panaccione, M L Apicella, G Calabrò, C Cianfarani, D Frigione, G Mazzitelli, C Mazzotta, V Pericoli, F Santini, A A Tuccillo, O Tudisco, and the FTU Team, to be published in Nature c. (2010)
[9]. Challis C., Plasma Physics and Controlled Fusion **44** (2002) 1031–1055[Diem 2009] S. J.
[10]. Diem, G. Taylor, J. B. Caughman, P. C. Efthimion, H. Kugel, B. P. LeBlanc, C. K. Phillips, J. Preinhaelter, S. A. Sabbagh and J. Urban, Physics Review Letters, **103** (2009) 015002
[11]. Ekedahl A et al. Plasma Physics and Controlled Fusion **51** (2009) 044001 (17pp)
[12]. Fisch., Physics Review Letters, **41**, 873(1978) & erratum **42**, 410(1979)
[13]. Fisch., Physics Review Letters, **45**, 720 (1980)
[14]. V. Fuchs, M. Goniche, Y. Demers, P. Jacquet and J. Mailloux, Physics of Plasmas **3**, 4023 (1996).
[15]. V. Fuchs et al., 37th Conference on Plasma Physics, Dublin, 21-25 June 2010, P2-130
[16]. J. Garcıa, G. Giruzzi, J. F. Artaud, V. Basiuk, J. Decker, F. Imbeaux, Y. Peysson, and M. Schneider, Phys. Physics Review Letters, **100** (2008) 255004
[17]. J. Garcia, G. Giruzzi, P. Maget, J.F. Artaud, V. Basiuk, J. Decker, G. Huysmans, F. Imbeaux, Y. Peysson, M. Schneider, Nucl. Fusion 50 (2010) 025025.
[18]. M.Goniche et al., Nuclear Fusion, **28** (1998) 919
[19]. M.Goniche et al., 16th Topical Conference on Radio Frequency Power in plasmas, Park City, Utah, U.S.A., 11-13 April, 2005
[20]. M. Goniche, A. Ekedahl, K. Rantamäki,, V.Petrzilka, G. Arnoux, 690, L. Delpech, P. deVries, K. Erents, S. Jachmich, M. Mayoral, J. Ongena, K. Zastrow, 22nd IAEA Fusion Energy Conference, EXP/P6-22, 13-18 Octobre 2008 , Genève
[21]. Goniche M. et al., Plasma Physics and Controlled Fusion **51** (2009) 044002 (18pp)
[22]. Green B.J. et al 2003 Plasma Physics and Controlled Fusion **45** 687
[23]. R. W. Harvey and M. McCoy. The CQL3D Fokker-Planck Code. Proceedings of the IAEA Technical Committee Meeting on Simulation and Modeling of Thermonuclear Plasmas, pages 489–526, 1992.
[24]. J.Hillairet et al., Fusion Engineering and Design, **84** (2009) 953-955
[25]. Hoang G.T., Nuclear Fusion, **49** (2009) 07500 (11pp)
[26]. W. Hooke, Plasma Physics and Controlled Fusion **26** (1984) 133
[27]. Ikeda Y et al., in Controlled Fusion and Plasma Physics (Proc. 15th Int. Conf., Sevilla, 1994, p.415)
[28]. [ITER physics basis 99] ITER physics expert group on energ. particles, heating and current drive, Nuclear Fusion, **39** (1999) 2495
[29]. Joffrin E., Plasma Physics and Controlled Fusion 45 (2003) A367–A383
[30]. Karney Physics ofFluids, **28** (1985) 116-126
[31]. K.K. Kirov, Yu. Baranov, J. Mailloux, M.-L. Mayoral, M.F.F. Nave, J. Ongena and JET EFDA Contributors, Nuclear Fusion **50** (2010) 075003 (17pp)
[32]. Litaudon X., Nuclear Fusion **47** (2007) 1285–1292

[33]. A. Loarte, et al., Proc. 22nd IAEA Fusion Energy Conf., IT/P6-13 (2008)
[34]. Mailloux J., Physics of Plasmas, **9** (2002) 2156-2164
[35]. D.Moreau, Plasma Physics, Vol. **23** (1981)15-21
[36]. Nguyen the Hung and Wersinger J. M., Helvetica Physica Acta, **48** (1975) 465
[37]. Pericoli Ridolfini, Nuclear Fusion, **34** (1994) 469
[38]. Pericoli RidolfiniV, G. Calabro, L. Panaccione, FTU team and ECH team, Nucl. Fusion 45 (2005) 1386–1395
[39]. Pericoli RidolfiniV. Pericoli Ridolfini,
[40]. Y.Peysson, J.Decker, AIP Conf. Proc., September 28, 2007, Volume 933, pp. 293-296, Radio Freq. Power in Plasmas, 17th Top. Conf. on Radio Freq. Power in Plasmas
[41]. Y. Peysson, J. Decker, Physics of Plasmas, **15**, 092509 (2008) 14pp
[42]. P.Platania, 37th Conference on Plasma Physics, Dublin, 21-25 June 2010, P.128
[43]. Porkolab M. Physics ofFluids **20** (1977) 2058
[44]. Porkolab M., Bernabei S., Hooke W.M. et al., Physical Review Letters, **38** (1977) 230
[45]. Tripathi V.K., Liu C.S. and Grebogi C. 1979 Physics of Fluids **22**
[46]. Sharma P.K. et al., 37th Conference on Plasma Physics, Dublin, 21-25 June 2010, P5-184
[47]. C.Sozzi et al., AIP Conf. Proc., vol. 988, (2008) 73.
[48]. Tuccillo A.A. et al., Plasma Physics and Controlled Fusion, **47** (2005) B363–B377
[49]. K.Ushigusa et al., Plasma Physics and Controlled Fusion, **38** (1996) 1825
[50]. K.Ushigusa et al., Fusion Science and Technology **42** (2002)255-277
[51]. Wallace G., PhD thesis, 2010, MIT, USA
[52]. Wright, J.C., Bonoli, P.T., Schmidt, A.E., Phillips, C.K., Valeo, E.J., Harvey, R.W., and Brambilla, M.W, Physics of Plasmas **16**, 072502 (2009).

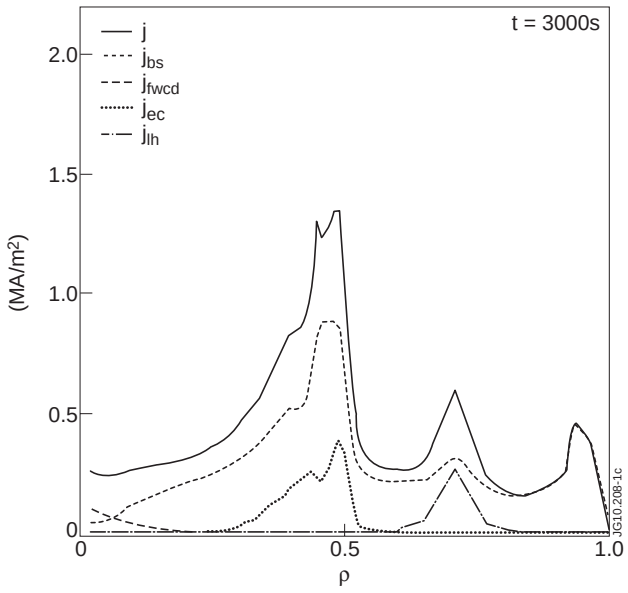

Figure 1: SS scenario for ITER: current profiles from the different sources [16].

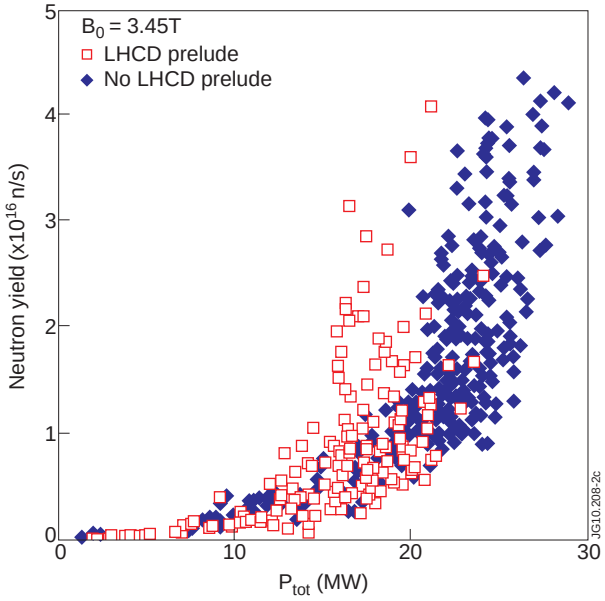

Figure 2:Neutron yield of discharges JET discharges with and without LHCD prelude [9].

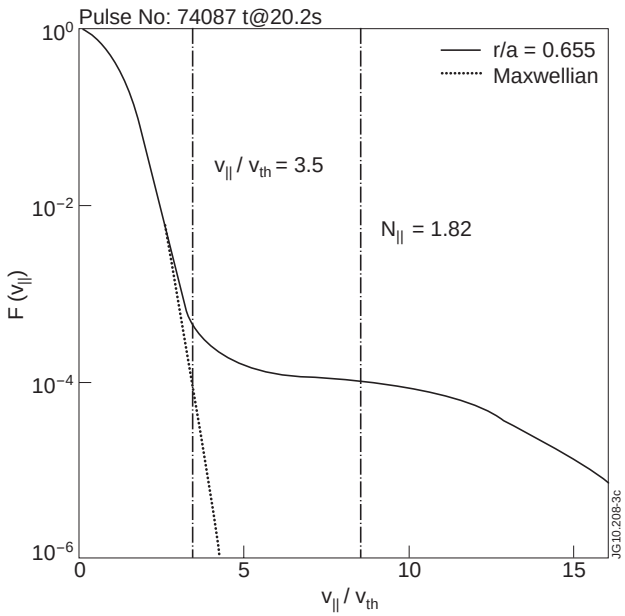

Figure 3: Modelling of the electron distribution function of a JET pulse (P_{LH} = 5MW, $N_{//,launched}$ = 1.82, $\overline{n}_e$ = $2.9\times10^{19}m^{-3}$) from the 3D C3PO/LUKE ray tracing/ Fokker-Planck code [40].

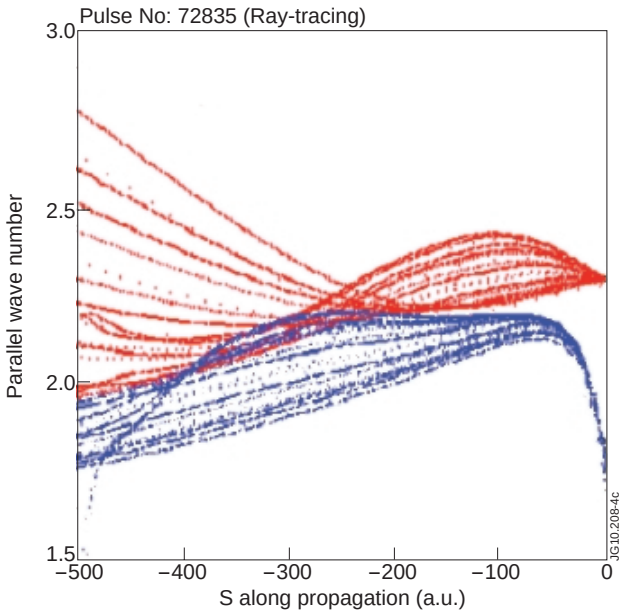

Figure 4: $N_{//}$ along the propagation (right to left) from the 3D RAYSTAR ray tracing code [4] for JET steady-state scenario Pulse No: 7283. Launched rays are in red, the minimum $N_{//}$ for wave accessibility in blue.

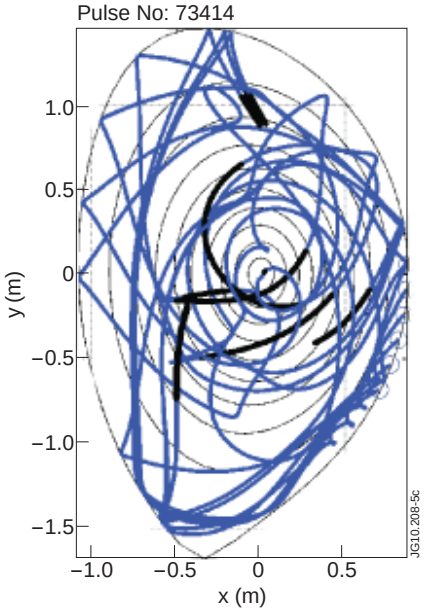

Figure 5: Poloidal projection of the ray tracing from the C3PO ray tracing code for JET Pulse No: 73417. The thicker ray portions (in black) identify regions of strong power absorption.

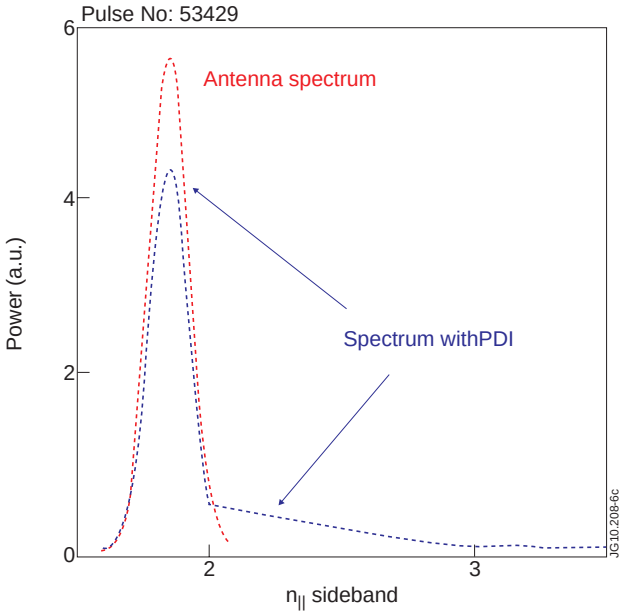

Figure 6: Computed spectral broadening for low density SS scenario JET pulse.

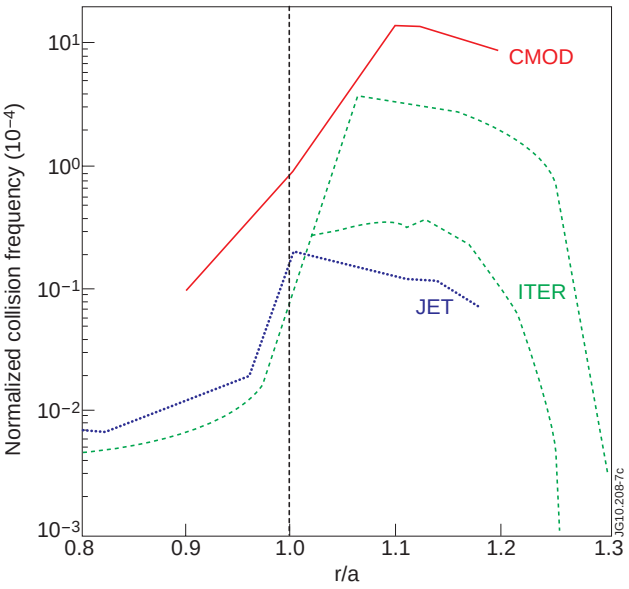

Figure 7: Normalized electron-ion collision frequency ν/f for JET, C-Mod and ITER

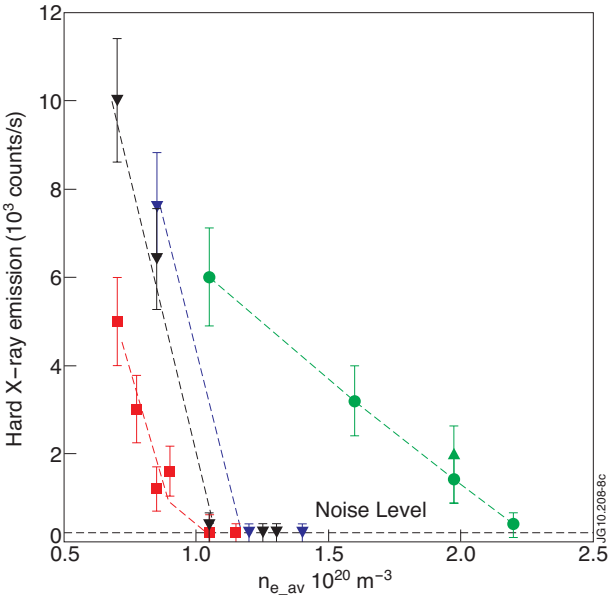

Figure 8: HXR emission for the low T_e (red, black and blue symbols for different plasma currents and magnetic fields) and high T_e (green symbols) regime on FTU [8].

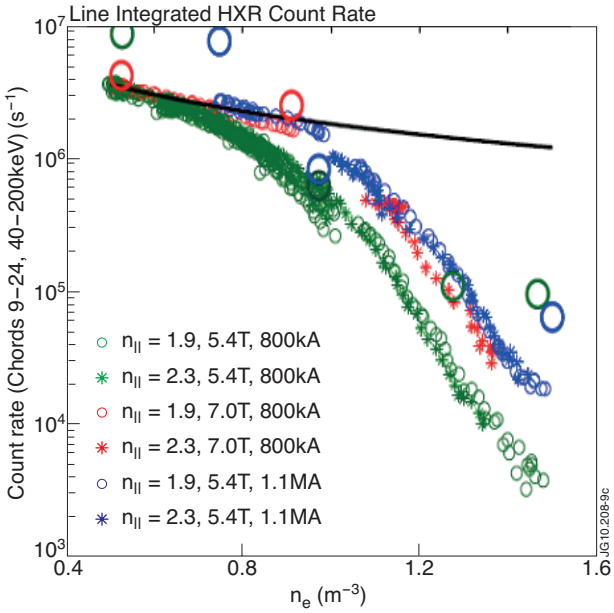

Figure 9: HXR emission on C-Mod. The large symbols represent simulations including collisional damping while the small symbols are experimental data. The simulation without collisional damping roughly follows the solid line ($1/\bar{n}_e$) [51].

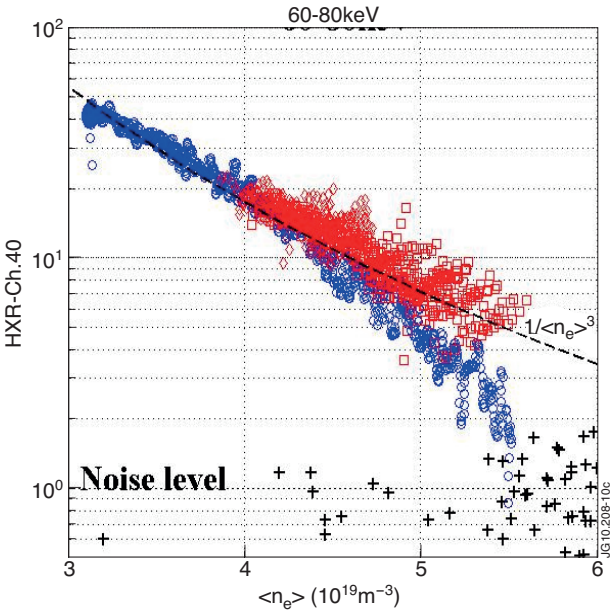

Figure 10: HXR emission on Tore Supra (B_t = 3.85T, I_p = 1MA, P_{LH} = 2MW) for gas (circles) and pellets (squares) fuelling.

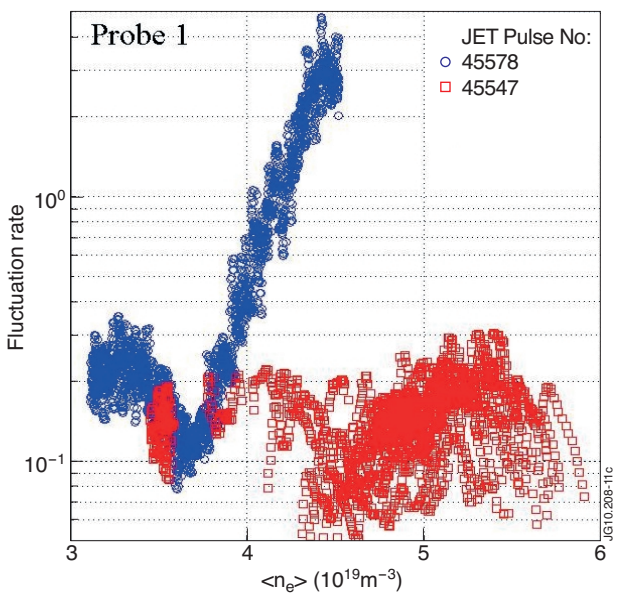

Figure 11: Fluctuation rate $\delta I_{sat}/I_{sat}$ for the same two discharges of figure 10. For Pulse No: 45578 (gas fuelling), the measurement is saturated when $<n_e> > 4.5\times10^{19}\ m^{-3}$.

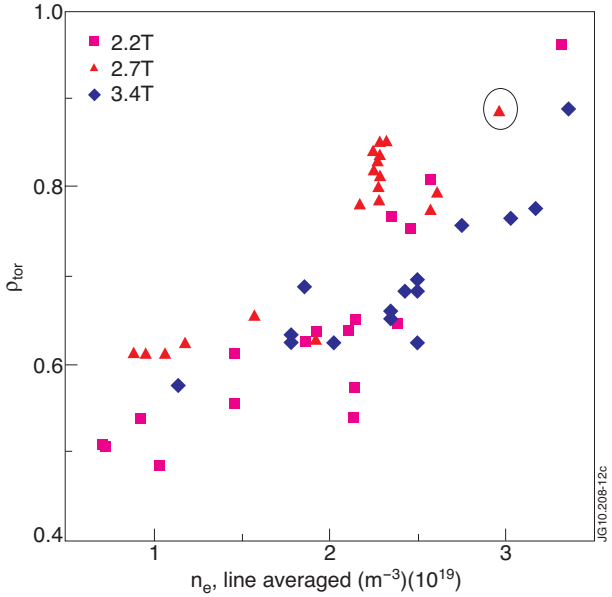

Figure12: Normalized radius of LH power deposition on JET from LH power modulation experiment. The circled point is for a pulse with conditions close to that of the SS scenario case but with lower density [31].

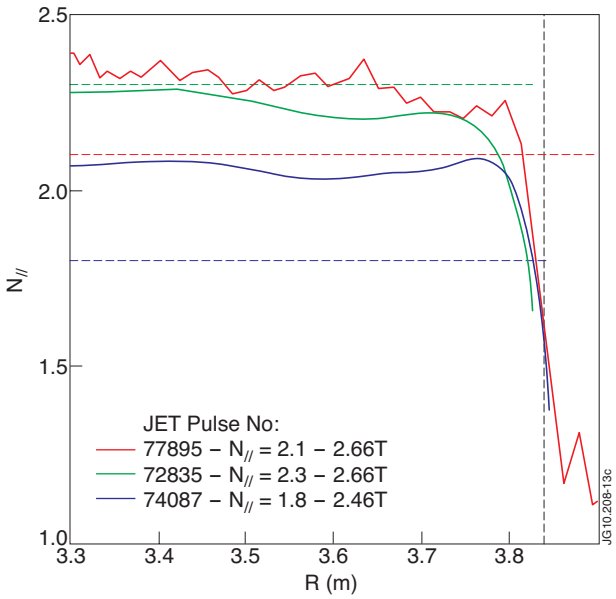

Figure 13. Minimum $N_{//}$ for wave accessibility for 3 pulses. The launched $N_{//}$ is indicated with a dashed line.

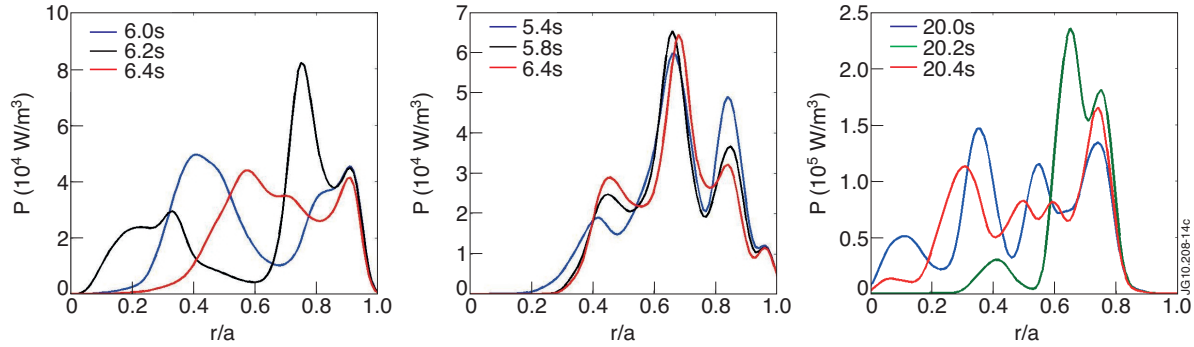

Figure14. Power deposition for three JET Pulse No's: (a) 77895 ($N_{//}$ = 2.1, high density), (b) 72835 ($N_{//}$ = 2.3, high density), (c) Pulse No: 74087 (($N_{//}$ = 1.8, medium density).

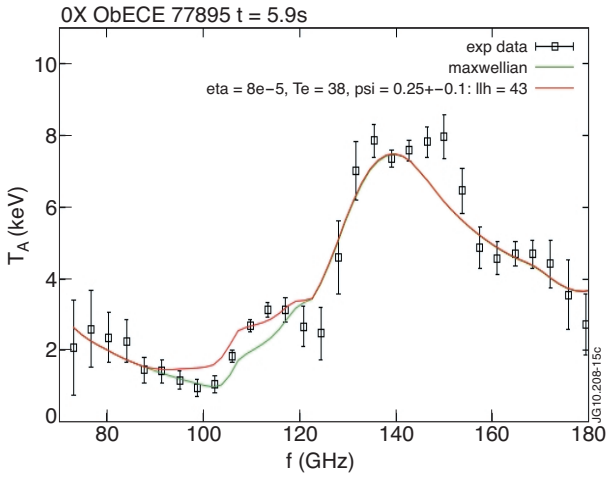

Figure 15: ECE spectrum for JETPulse No: 77895. Experimental points (symbols), modelled signal with no LH tail (blue solid line), with a LH tail (red dashed line).

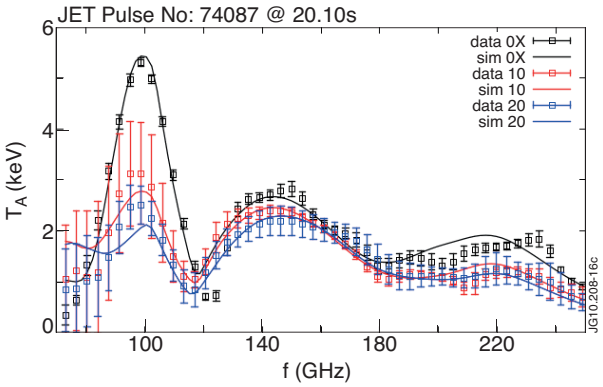

Figure 16: ECE spectra for JETPulse No: 74087 (3 lines-of-sight). Experimental points (symbols), modelled signals with a LH tail (solid lines).

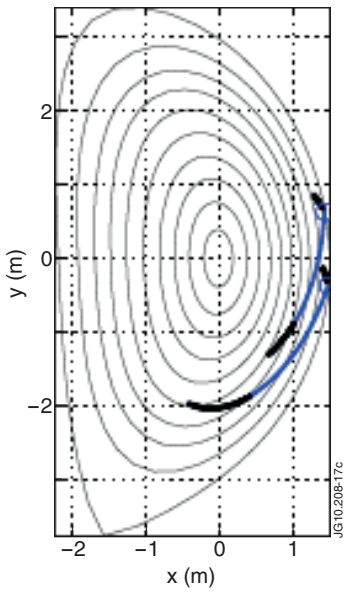

Figure 17: Ray tracing (poloidal cut view) for the SS scenario of ITER. F=5GHz, $N_{//}$ = 1.95. The thicker ray portions identify regions of strong power absorption (C3PO code).